Mechanism of Aldose Reductase Inhibition: Binding of $NADP^+$/NADPH and Alrestatin-like Inhibitors†

Torsten Ehrig,‡ Kurt M. Bohren,§ Franklyn G. Prendergast,‡ and Kenneth H. Gabbay*,§,‖

Department of Biochemistry and Molecular Biology, Mayo Foundation, Rochester, Minnesota 55905, and Molecular Diabetes and Metabolism Section, Departments of Pediatrics and Cell Biology, Baylor College of Medicine, Houston, Texas 77030

Received February 3, 1994; Revised Manuscript Received April 8, 1994®

ABSTRACT: Aldose reductase enfolds $NADP^+$/NADPH via a complex loop mechanism, with cofactor exchange being the rate-limiting step for the overall reaction. This study measures the binding constants of these cofactors in the wild-type enzyme, as well as a variety of active-site mutants (C298A, Y48H, Y48F, Y209F, H110A, W219A, and W20A), and seeks to identify the binding site and mechanism of the aldose reductase inhibitor alrestatin in the recombinant human enzyme. All the mutant enzymes, regardless of their enzyme activities, have normal or only slightly elevated coenzyme binding constants, suggesting a tertiary structure similar to that of the wild-type enzyme. Binding of alrestatin was detected by fluorescence assays, and by an ultrafiltration assay which measures the fraction of unbound alrestatin. Alrestatin binds preferentially to the enzyme/$NADP^+$ complex, consistent with the steady-state inhibition pattern. Alrestatin binding and enzyme inhibition were abolished in the Tyr48 mutants Y48F and Y48H, implicating the positively charged anion well formed by the $Asp43^-$/$Lys77^+$/$Tyr48^0$/$NADP^+$ complex in inhibitor binding (Harrison et al., 1994; Bohren et al., 1994). The enzyme mutant W20A severely affected the inhibitory potencies of a variety of commercially developed aldose reductase inhibitors (zopolrestat, tolrestat, FK366, AL1576, alrestatin, ponalrestat, and sorbinil). Inhibition by citrate, previously shown to bind to the positively charged anion well, was not affected by this mutation. Inhibitors with flexible double aromatic ring systems (zopolrestat, FK366, and ponalrestat) were less affected than others possessing a single aromatic ring system, suggesting that the additional pharmacophor ring system stabilizes the inhibitor by interaction at some other hydrophobic site. These findings indicate that the inhibitors require a negative charge to anchor to the anion well, and stacking of their aromatic ring systems against the Trp20 residue in the active site to stabilize and increase the avidity of binding.

Aldose reductase is a monomeric enzyme that catalyzes the reduction of a wide variety of aldehydes using NADPH as a coenzyme. It shares structural similarity and substrate specificity with members of the aldo–keto reductase superfamily (Wermuth, 1985; Bohren et al., 1989). The enzyme is implicated in the pathogenesis of a variety of diabetic complications (Gabbay, 1973; Kinoshita, 1974; Kador, 1988), which has been the rationale for efforts to develop effective aldose reductase inhibitors (Dvornik, 1987).

The crystal structure and catalytic mechanism of the enzyme were elucidated recently. Aldose reductase is an α/β barrel enzyme (Rondeau et al., 1992) with the NADPH cofactor enfolded across the C-terminal end of the barrel by a loop of residues (Wilson et al., 1992). The 4-*pro-R* hydrogen of the nicotinamide is exposed to solvent at the bottom of an active-site pocket lined with hydrophobic residues, some of which are contributed by the loop enfolding the NADPH (Wilson et al., 1992; Harrison et al., 1994). Two residues, His110 and Tyr48, along with the 4-*pro-R* hydrogen of the nicotinamide, form a triangle at the bottom of the active-site pocket. An explanation of the substrate binding and catalytic mechanism was provided by the identification of the carboxylate moiety of citrate bound at the center of the plane of this equilateral triangle, and the determination that the crystal-bound cofactor is $NADP^+$ (Harrison et al., 1994). This anion well was also found to bind other anions such as cacodylate and phosphate. His110 was shown to direct substrate stereochemical selectivity, and Tyr48 to be the proton donor in the reduction mechanism (Bohren et al., 1994). Tyr48 is perturbed by the adjoining Asp43/Lys77 residues which impart to it a lower pK_a. Citrate inhibits aldose reductase, and in common with other negatively charged aldose reductase inhibitors (e.g., alrestatin, sorbinil, zopolrestat, etc.) is an uncompetitive to noncompetitive inhibitor with respect to aldehyde substrates in the forward direction, and a competitive inhibitor with respect to the alcohol in the backward reaction; i.e., they bind the $NADP^+$ form of the enzyme (Harrison et al., 1994). The inhibitor binding site is thus a positively charged anion well formed by Tyr48, His110, and the nicotinamide ring (Harrison et al., 1994). A recent structural study (Wilson et al., 1993) described the aldose reductase inhibitor zopolrestat bound to the holoenzyme, which shows the carboxylate moiety of zopolrestat binding to the anion well identically to citrate and the other anions, thus confirming the importance of the anion well in binding this class of inhibitors.

The catalytic mechanism of aldose reductase involves binding of the substrate to the active-site pocket of the enzyme/NADPH complex with subsequent hydride transfer from the nicotinamide ring to the carbonyl group. A proton is donated by Tyr48 to the carbonyl oxygen to complete the conversion

† This work was supported by NIH Grant GM34847 (F.G.P.), Juvenile Diabetes Foundation grants (K.M.B. and K.H.G.), a Thompson-Mayo fellowship (T.E.), and the Harry B. and Aileen B. Gordon Foundation (K.H.G.).

* Address correspondence to this author at the Departments of Pediatrics and Cell Biology, Baylor College of Medicine, 1 Baylor Plaza, Houston, TX 77030. Telephone: (713) 770-3765. FAX: (713) 770 3766. Internet: kgabbay@mbcr.bcm.tmc.edu.

‡ Mayo Foundation.

§ Department of Pediatrics, Baylor College of Medicine.

‖ Department of Cell Biology, Baylor College of Medicine.

® Abstract published in *Advance ACS Abstracts,* June 1, 1994.

0006-2960/94/0433-7157$04.50/0

of the aldehyde to alcohol. The hydride transfer step is more rate-limiting than proton transfer (Bohren et al., 1994), while the cofactor exchange and its attendant loop and enzyme conformational changes appear to be the rate-limiting step for the overall enzymatic reaction (Grimshaw et al., 1989; Kubiseski et al., 1992).

In the present study, we have determined the binding of NADPH and $NADP^+$ as well as an aldose reductase inhibitor, alrestatin, to the wild-type enzyme and several other mutant enzymes with mutations of specific active-site residues. The results indicate that aldose reductase inhibitor binding within the active-site pocket requires a negatively charged group (carboxylate or spirohydantoin) anchored to the anion well formed by the $Asp43^-/Lys77^+/Tyr48^0/NADP^+$ complex, and stacking of an aromatic ring system against Trp20. Thus, the oxidation state of the cofactor in the enzyme/coenzyme complex is critical to the initial binding of this class of inhibitors, and the aromatic ring system(s) crucial to the avidity of binding.

MATERIALS AND METHODS

Chemicals. Alrestatin was obtained from Ayerst Laboratories, and tolrestat was obtained from its successor, Wyeth-Ayerst. Sorbinil and zopolrestat (Pfizer), ponalrestat (ICI), FK366 (Fujisawa), and AL1576 (Alcon) were kindly provided by colleagues and collaborators. Dithiothreitol (DTT)[1] was purchased from Boehringer-Mannheim, Indianapolis, IN. All other chemicals were purchased from Sigma, St. Louis, MO.

Expression, Mutagenesis, and Purification of Enzymes. Aldose reductase was expressed in *Escherichia coli* as described previously (Bohren et al., 1991). Site-directed mutagenesis was performed with the Amersham mutagenesis kit in single-stranded M13 using oligomers with the required mismatches, and the mutated cDNA was subcloned into the pET 11a vector (Novagen, Madison, WI) for expression as previously described (Bohren et al., 1991). The oligonucleotides for site-directed mutagenesis and production of the C298A, Y48H, Y48F, and H110A mutant enzymes were previously described (Bohren & Gabbay, 1993; Bohren et al., 1994). Site-directed mutagenesis to produce the Y209F, W219A, and W20A mutant enzymes used the following oligonucleotides, respectively: 5′GGTGACCGCCTTCAGCCCCCTCG′3; 5′-CTGACAGGCCCGCGGCCAAGCCCGAGG′3; and 5′GT-TGGGTACCGCGAAGTCCCCTC′3.

The expressed proteins were treated by one of two methods to produce nucleotide-free enzyme. In method 1, the protein was initially purified by DEAE-Sephacel chromatography (Pharmacia) and subsequently chromatographed on a column of Matrex Orange A (Amicon, Danvers, MA) with elution by NADPH as previously described (Bohren et al., 1991). The NADPH was removed from the enzyme as follows: the enzyme/coenzyme complex, contained in 2 mL of 5 mM phosphate/100 μM DTT, pH 7.0, buffer (buffer A), was made 0.6 M in ammonium sulfate by the addition of a 4 M stock solution. The mixture was incubated for 3 min and loaded on a 1 × 50 cm Biogel P-10 column (Bio-Rad, Richmond, CA) equilibrated with buffer A. The column bed was primed with 3 mL of 0.6 M ammonium sulfate in buffer A immediately before loading the enzyme. The enzyme was chased with 3 mL of 0.6 M ammonium sulfate in buffer A, followed by buffer A. In method 2, the coenzyme-free aldose reductase was prepared *de novo* by eluting the enzyme from the Matrex Orange A column with 0.5 M NaCl in buffer A, instead of NADPH. The salt concentration in the sample was subsequently reduced to 5 mM by washing the protein with buffer A in an Amicon concentrator equipped with a YM-5 membrane. The two methods yielded enzymes free of coenzyme as judged by the recovered coenzyme during gel filtration, from the shift of the protein absorbance peak from 265 nm (holoenzyme) to 280 nm (apoenzyme), and from the absence of the NADPH absorbance band at 340 nm. Enzyme activity was routinely measured in 100 mM phosphate buffer, pH 7.0, containing 100 μM NADPH and a saturating concentration of DL-glyceraldehyde. The oxidation of NADPH was followed spectrophotometrically by measuring the decrease in absorbance at 340 nm. Mutants with weak or no enzymatic activity were detected during the purification procedure by SDS–PAGE, using precast 10–15% gradient gels on the Phastsystem (Pharmacia, LKB Biotechnology) in the presence of 2% β-mercaptoethanol as described by the manufacturer.

Enzyme Characterization. The purified enzyme protein concentration was determined from the absorbance at 280 nm. The extinction coefficient was estimated from the known amount of tryptophan and tyrosine residues in the enzyme (Bohren et al., 1989) assuming an extinction coefficient of 5690 M^{-1} cm^{-1} for each tryptophan residue, and of 1280 M^{-1} cm^{-1} for each tyrosine residue (Gill & von Hippel, 1989). An extinction coefficient of 50 500 M^{-1} cm^{-1} was calculated for the wild-type enzyme, and correspondingly lower values for mutants with tyrosine or tryptophan substitutions.

The concentration of active sites was determined by titrating a high concentration (5 μM) of protein with NADPH, the binding of which was followed by the quenching of protein fluorescence. The excitation and emission wavelengths of 295 and 373 nm, respectively, were chosen at the edges of the major absorption bands of NADPH to avoid an inner filter effect. Due to the tight binding of NADPH, a titration curve with an inflection point is obtained, and the concentration of active sites equals the NADPH concentration at this point.

Steady-State Enzyme Kinetics. Steady-state kinetic constants and their standard errors were calculated by fitting the Michaelis–Menten function directly in the hyperbolic form to the data with an unweighted least-squares analysis using the Marquardt–Levenberg algorithm provided with SigmaPlot, version 5.0. Initial rates in the presence of inhibitors were analyzed by using eq 1 where K_{is} is the slope (competitive)

$$v_i = VA/[K_m(1 + I/K_{is}) + A(1 + I/K_{ii})] \qquad (1)$$

inhibition constant, K_{ii} is the intercept (uncompetitive) inhibition constant, V is the maximal velocity, A is the substrate concentration, I is the inhibitor concentration, and K_m is the Michaelis–Menten constant. The inhibition pattern and a >100-fold relative difference between K_{is} and K_{ii} determined competitive ($K_{ii} \gg K_{is}$) or pure noncompetitive inhibition if K_{is} and K_{ii} were not significantly different ($K_{is} \sim K_{ii} = K_i$).

Spectroscopic Measurements. Fluorescence spectra and single-wavelength emission intensities were measured on a Perkin-Elmer FP66 or a Spex Fluorolog fluorometer in 1-mL cuvettes at a temperature of 20 °C. The absorbances of protein, coenzymes, and alrestatin were measured on a Cary 2200 or a Gilford Response spectrophotometer at 20 °C. Absorbance spectra of enzyme-bound $NADP^+$ were obtained by digitally subtracting the absorbance of ligand-free enzyme from that of the enzyme–$NADP^+$ complex.

Determination of Coenzyme Binding. Titrations with coenzyme were done at a protein concentration of between

[1] Abbreviations: SDS, sodium dodecyl sulfate; PAGE, polyacrylamide gel electrophoresis; DTT, dithiothreitol.

0.07 and 1.2 μM in 5 mM sodium phosphate, pH 7.0, containing 100 μM DTT. The formation of enzyme/coenzyme complex was followed by extensive quenching of protein fluorescence upon addition of coenzymes. A Perkin-Elmer MPF66 fluorometer with excitation and emission wavelengths set at 295 and 373 nm, respectively, was used. The fractional saturation (α) by coenzyme of the total coenzyme binding sites, was equated to the ratio $\Delta F/\Delta F_{max}$ (eq 2), where ΔF

$$\alpha = \Delta F/\Delta F_{max} \quad (2)$$

is the amount of fluorescence reduction at a specified coenzyme concentration and ΔF_{max} is the limiting amount of fluorescence reduction at fully saturating coenzyme concentration. ΔF_{max} was in all cases reached at coenzyme concentrations of 9 μM, at which point no further drop in fluorescence upon addition of coenzyme was observed. Since aldose reductase binds coenzymes very tightly, the depletion of ligand during the titration had to be taken into account. Therefore, the dissociation constant was evaluated by a variation of the Scatchard plot as described by Stinson and Holbrook (1973). Briefly, this method relates the fractional saturation α to the total concentration of ligand, L_0, by the equation where E_0 is

$$L_0/\alpha = K_d/(1-\alpha) + E_0 \quad (3)$$

the total active-site concentration and K_d the dissociation constant. A plot of $1/(1-\alpha)$ versus L_0/α yields a theoretically straight line for a homogeneous ligand receptor, with the slope equal to the binding constant and y-axis intercept equal to the concentration of binding sites (Stinson & Holbrook, 1973). Standard errors of the slope (K_d) were calculated using SigmaPlot, version 5.0.

Determination of Alrestatin Binding by Fluorescence Titration. Binding of alrestatin to aldose reductase was followed by a change in alrestatin fluorescence emission intensity during titration with alrestatin. To avoid an inner filter effect from the absorbance of alrestatin (maximal absorption at 340 nm which corresponds to the excitation band maximum in Figure 1D), the excitation wavelength was set at 373 nm. The emission was read at 390 nm. This emission wavelength avoids interference from the fluorescence of NADPH which emits only at longer wavelengths (Figure 1C). The binding constant was estimated from the dependence of the fractional saturation α on the ligand concentration L_0 by the modified Scatchard plot as described above.

Determination of Alrestatin Binding by Ultrafiltration Assays. The binding of alrestatin to aldose reductase was also directly assessed by determining the unbound fraction of alrestatin. A spun microconcentrator with a molecular mass cutoff of 3000 Da (Centricon 3; Amicon, Danvers, MA) was used to separate the free from the enzyme-bound alrestatin. Since alrestatin adsorbs significantly to the ultrafiltration membrane, the membrane was preadsorbed by filtering 0.5 mL of a 5 μM alrestatin solution through the membrane. A volume of 1 mL of binding assay mixture was then added to the upper chamber of the concentrator, and approximately 100 μL was filtered through the membrane. The filtrate was diluted 10-fold with 5 mM phosphate, pH 7.0, and the concentration of alrestatin was determined by fluorometry using excitation and emission wavelengths of 340 and 380 nm, respectively. Due to the preadsorption with alrestatin, a small amount of this substance was bleeding from the membrane in control assays where only buffer was loaded into the upper chamber (about 0.5 μM was found in the filtrate). The concentration of alrestatin in the filtrate from the binding assays was corrected accordingly. The binding assay contained 12 μM enzyme active sites, 5 μM alrestatin, and either no coenzyme or 10 μM $NADP^+$ or NADPH, according to the binding conditions tested. The buffer was 5 mM phosphate, pH 7.0, containing 100 μM DTT, and the binding temperature was 25 °C.

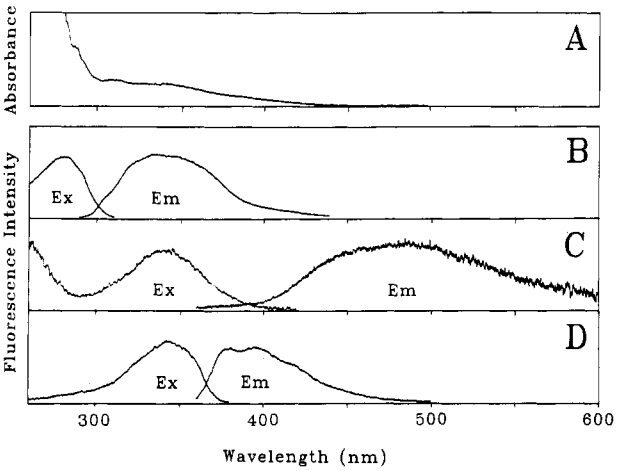

FIGURE 1: Spectral overlaps of components used in spectroscopic assays. (A) Absorbance spectrum of $NADP^+$ bound to wild-type aldose reductase. The spectrum of coenzyme-free enzyme was subtracted from that of an equal concentration of enzyme in the presence of a saturating concentration of $NADP^+$. (B–D) Fluorescence excitation and emission spectra of coenzyme-free wild-type aldose reductase protein (B), NADPH (C), and alrestatin (D). All spectra were obtained in 5 mM phosphate buffer, pH 7.0, containing 100 μM DTT. The y-axes are arbitrarily scaled.

The need to preadsorb the membrane with alrestatin, and the resulting bleeding of alrestatin from the membrane, although it was small and could be corrected for, precludes derivation of the binding constants from ultrafiltration assays. However, these assays are quite adequate as a semiquantitative method to determine whether the absence of a spectroscopic effect in the alrestatin fluorescence titration assays is a *bona fide* failure to bind alrestatin, or due to a failure of bound alrestatin to produce a spectroscopic effect.

RESULTS

Characterization of Enzymes. All the enzymes were readily purified and yielded single bands on SDS–PAGE (not shown). All the enzymes listed exhibited enzymatic activity except for the Y48F mutant which is inactive (Bohren et al., 1994). The molar ratio of active-site concentration (determined by nucleotide binding) to protein concentration ranged between 0.75 and 0.85 for the wild-type and other mutant enzymes. The Y48F mutant was an exception in that this ratio was only 0.50, suggesting the presence of some immature or improperly folded Y48F protein (see below).

Spectral Overlaps of Cofactors, Alrestatin, and Aldose Reductase. The titration studies make use of the extensive quenching of aldose reductase protein fluorescence upon binding of the coenzyme, and of the quenching of alrestatin[2] fluorescence upon binding to the enzyme:nucleotide complex. Figure 1 shows that these quenching phenomena can, at least in part, be explained by resonance energy transfer since there are favorable spectral overlaps of a donor fluorescence emission band with an acceptor excitation band. There is an extensive

[2] Alrestatin was chosen for these studies as the only one among several aldose reductase inhibitors examined [sorbinil (Pfizer), tolrestat (Wyeth-Ayerst), ponalrestat/statil (ICI), FK366 (Fujisawa), AL1576 (Alcon)] that showed fluorescence characteristics permitting these studies.

Table 1: Coenzyme (NADP+/NADPH) and Inhibitor Binding to Aldose Reductase[a]

enzyme	K_d(NADP) (nm)	K_d(NADPH) (nM)	K_d(alrestatin) (μM)	IC_{50} (μM)	NADPH fluorescence intensity[b]	ϵ[c] Racker band
wild-type	6	10	0.3	1	0.40	1.7
C298A	60	30	0.3	3	0.50	
Y48H	10	2.4	no binding	*d*	1.10	
Y48F	17	46	no binding	*e*	4.9	4.4
Y209F	8	25	no sat.[g]	3	0.62	
H110A	24	7	no sat.	42	4.50	1.6
W219A	22	36	no sat.	25	0.54	2.4
W20A	28	58	no binding	n.i.[f]	7.4	0.77

[a] Binding assays were in 5 mM phosphate, pH 7.0, buffer, with 100 μM DTT, at 20 °C. Alrestatin binding constants were determined in the presence of a saturating concentration of NADP+. Binding constants were determined according to Stinson and Holbrook (1973). Standard errors of K_d <20%. [b] Ratio of the fluorescence emission intensity of bound NADPH to that of an equal concentration of unbound NADPH. The excitation wavelength was 340 nm, and the emission was read at the wavelength of maximal fluorescence. [c] ϵ is the extinction coefficient of the Racker band in 10^3 M^{-1} cm^{-1}. [d] 20% inhibition at 100 μM alrestatin concentration. [e] The Y48F enzyme is enzymatically inactive. [f] ni = no inhibition. [g] no sat. = binding saturation was not reached and K_d could not be calculated.

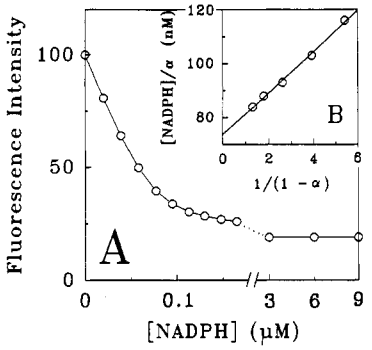

FIGURE 2: Titration of wild-type aldose reductase enzyme with NADPH. (A) Protein fluorescence intensity at different NADPH concentrations. Excitation and emission wavelengths were 295 and 373 nm, respectively. The assay contained 0.11 μM protein in 5 mM phosphate buffer, pH 7.0, with 100 μM DTT. (B) Replot of the data in panel A according to eq 3 (see text).

overlap between the fluorescence emission band of nucleotide-free aldose reductase protein (Figure 1B) and the excitation band of NADPH (Figure 1C), and also between the protein fluorescence emission band (Figure 1B) and the NADP+ charge-transfer absorbance band (Figure 1A). NADP+ alone does not absorb above 300 nm, and there is thus only minimal overlap with the protein emission band.

Binding of NADP+ to aldose reductase leads to the appearance of a charge-transfer absorbance band (Racker band, Figure 1A; Racker & Krimsky, 1952) with an extinction coefficient of 1700 M^{-1} cm^{-1} at 340 nm in the wild-type enzyme (Table 1). There is also a partial overlap of the fluorescence emission band of alrestatin (Figure 1D) with the excitation band of NADPH (Figure 1C) and with the NADP+ charge-transfer band (Figure 1A). These overlaps explain, at least in part, the quenching of the fluorescence of alrestatin upon binding to the enzyme/coenzyme complex.

Spectral Properties of Free and Bound Coenzymes. Table 1 shows that upon binding to the wild-type enzyme, the fluorescence emission intensity of NADPH is quenched to about 40% of the value for free NADPH. Binding to the enzyme depresses the absorbance of NADPH at 340 nm only slightly, to about 90% (not shown). Table 1 also shows that mutations of Tyr48, His110, and Trp20 lead to markedly enhanced (4.5–7.4-fold) rather than decreased fluorescence of NADPH upon binding. These mutants retain the charge-transfer band of bound NADP+ (Table 1), and its intensity is even enhanced in the Y48F mutant.

Binding Constants of Coenzymes. Figure 2A shows a typical titration curve of the stripped nucleotide-free wild-type enzyme with NADPH. Saturation is reached at high ligand concentrations (3–9 μM), and the resulting fluorescence depression corresponds to ΔF_{max} in eq 2. Figure 2B shows a replot of the first five titration points according to eq 2 to evaluate the binding constant. Occasionally, the leftmost point of such a replot deviated from linearity, possibly indicating heterogeneity of the enzyme preparation. Heterogeneity is a common finding in aldose reductase, and has been explained by its unusual redox behavior (Grimshaw et al., 1990a; Bohren & Gabbay, 1993). In evaluating the binding constant, such outlying single points were omitted and the binding constant was determined from the linear portion of the data points. The binding of both NADP+ and NADPH (forms of the coenzymes) is exceptionally tight with binding constants in the low nanomolar range for the wild-type enzyme (Table 1). The data show that in all the listed mutants the coenzyme binding constants are comparable to those determined for the wild-type enzyme. Specifically, the Y48F and Y48H mutants bind NADP+/NADPH quite well, which is consistent with proper folding of the enzyme peptide chain and normal geometry of the active-site pocket, previously shown for the crystal structure of the Y48H mutant (Bohren et al., 1994).

Enzyme Inhibition by Alrestatin. As was shown for other inhibitors, alrestatin displays a noncompetitive inhibition pattern with respect to the aldehyde substrate D-xylose when tested in the forward direction, i.e., reduction of aldehyde by NADPH (Figure 3A). In the backward direction, i.e., oxidation of the alcohol by NADP+, the pattern is competitive with respect to the alcohol substrate xylitol (Figure 3B). Fitting the experimental data to eq 1 yielded the apparent noncompetitive inhibition constants K_{is} (1.5 ± 0.3 μM) and K_{ii} (2.2 ± 0.2 μM) for the forward reaction, and the apparent competitive inhibition constant K_{is} (1.1 ± 0.1 μM) for the backward reaction (K_{ii} = infinite). Refitting eq 1 to the data for the forward reaction using the relationship for pure noncompetitive inhibition ($K_{ii} = K_{is} = K_i$) yielded a value of K_i = 2.0 ± 0.1 μM. The apparent nonlinear Lineweaver–Burk plot (Figure 3A), i.e., the downward curvature most noticeable at high concentration of alrestatin, is most likely due to the tight binding of alrestatin to the enzyme and/or to the concentration of enzyme used in the assay (0.5 μM) which was comparable to the alrestatin concentration (Morrison, 1969; Williams, 1979). The values of the calculated noncompetitive inhibition constants are therefore too high, and the true values are in the nanomolar range. Deviation from linearity due to tight binding of inhibitor or high enzyme concentration is not as readily discernible in the case of true competitive inhibition. Indeed, Figure 4B seems to represent classical competitive inhibition.

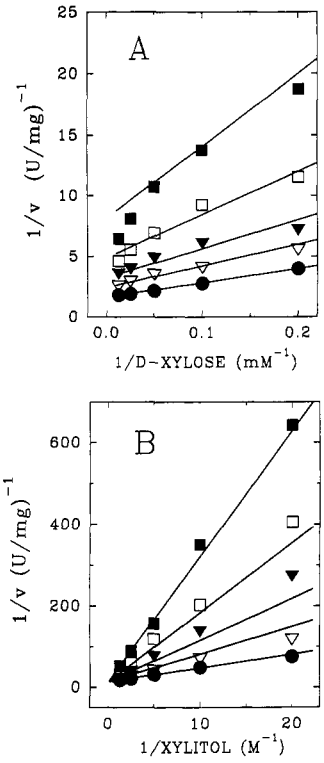

FIGURE 3: Inhibition of aldose reductase by alrestatin. (A) Noncompetitive inhibition of D-xylose reduction: alrestatin and D-xylose concentrations were varied (200 μM NADPH, pH 7.0); lines follow the fitted equation for pure noncompetitive inhibition: $v_i = VX/[K_m(1 + I/K_i) + X(1 + I/K_i)]$, whereby $K_i = 2.0 \pm 0.1$ μM, $K_m = 7.3 \pm 0.5$ mM. (B) Competitive inhibition of xylitol oxidation: alrestatin and xylitol concentrations were varied (200 μM NADP$^+$, pH 7.0); lines follow the fitted equation for competitive inhibition: $v_i = VX/[K_m(1 + I/K_{is})]$, whereby $K_{is} = 1.1 \pm 0.1$ μM, $K_m = 0.28 \pm 0.02$ M. Alrestatin concentrations: 0 (filled circles), 1 μM (open triangles), 2 μM (filled triangles), 4 μM (open squares), and 8 μM (filled squares).

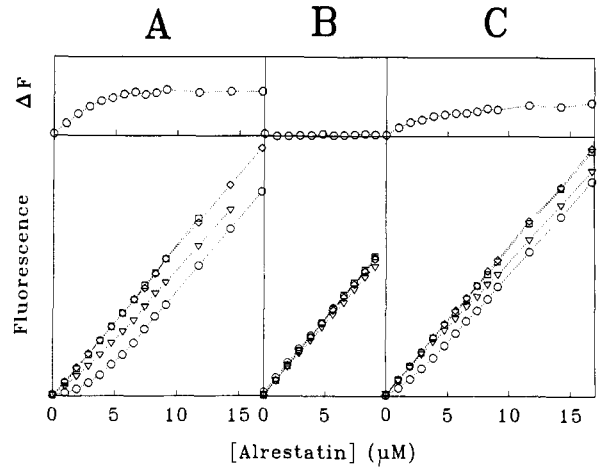

FIGURE 4: Titration of wild-type aldose reductase with alrestatin. (A) Wild-type aldose reductase; (B) Y48H mutant; and (C) H110A mutant. The fluorescence of alrestatin was determined at excitation and emission wavelengths of 373 and 390 nm, respectively. The enzyme active-site concentration was 3.3 μM, in 5 mM phosphate buffer, pH 7.0, containing 100 μM DTT. Alrestatin was titrated to the apoenzyme (squares), the enzyme/NADPH complex (triangles), the enzyme/NADP$^+$ complex (circles), and buffer (diamonds). The difference, ΔF, between the y-axis values for titration to the enzyme/NADP$^+$ complex and those for titration to buffer is shown for each enzyme in the upper panels.

The binding affinity of alrestatin to wild-type and active mutant enzymes (see below) correlated with their ability to be inhibited. Table 1 shows the concentration of alrestatin which inhibits the respective enzyme activity by 50% (IC_{50}) as well as the corresponding alrestatin binding constants. Binding of alrestatin was not detected by the spectroscopic method in either of the Y48 mutant enzymes, the inactive Y48F or the slightly active Y48H. Alrestatin did not bind to the W20A mutant and failed to inhibit its enzymatic activity. The relatively high IC_{50} value for H110A is partly due to the high concentration of enyzme used in the assay (10-fold increase in enzyme concentration relative to all other mutants tested) and in part due to the fact that H110 is an active-site residue. This latter explanation probably also applies to the slightly higher IC_{50} value for the W219A mutant enzyme. All IC_{50} values were determined under conditions where the coenzyme and the substrate (DL-glyceraldehyde) were saturating except in the case of the W20A mutant where inhibition by alrestatin was not detected. The K_m of W20A for DL-glyceraldehyde is 50 ± 2 mM, and saturation was not reached under the conditions used (100 mM DL-glyceraldehyde). Regardless, inhibition would only be stronger under such a condition (assuming K_{is} and K_{ii} are unequal), and as shown below, inhibition of the W20A mutant was impaired for all inhibitors tested (except citrate).

Binding of Alrestatin to Wild-Type Enzyme. The fluorescence of alrestatin is proportional to its concentration at the range used in these titrations. Titration of the enzyme/NADP$^+$ complex with alrestatin results in a deviation from this linearity, indicating quenching of the alrestatin fluorescence (Figure 4A). The initial additions of alrestatin lead to small increases in fluorescence due to enzyme binding, and upon saturation of the binding sites, each subsequent addition results in the same fluorescence increment as observed in the absence of enzyme. Subtraction of the enzyme/NADP$^+$ titration curve from that with buffer alone yields a saturation binding curve (Figure 4A, upper panel), where the fractional saturation, α, can be determined by eq 2 as described under Materials and Methods for titration with coenzyme. A plot according to eq 3 yields a binding constant of alrestatin to wild-type enzyme of 0.3 μM (Table 1). When alrestatin is titrated to the enzyme/NADPH complex, the quenching effect is only minimal, and for the apoenzyme, it is completely absent (Figure 4A, lower panel). These findings suggest that alrestatin binds best to the enzyme/NADP$^+$ complex, with weaker binding affinity to the enzyme/NADPH complex and practically none to the apoenzyme.

However, the absence of a quenching effect in the spectroscopic titrations could also result if alrestatin binds but does not produce a spectroscopic effect. We have therefore tested the binding of alrestatin to enzyme protein directly by determining the fraction of unbound alrestatin using ultrafiltration assays. These assays clearly confirm that alrestatin binds preferentially to the enzyme/NADP$^+$ complex as opposed to the enzyme/NADPH complex, with minimal binding to the nucleotide-free apoenzyme (Table 2).

Binding of Alrestatin to Aldose Reductase Mutants. Binding of alrestatin to the enzyme/NADP$^+$ complex of four of the active-site mutants (C298A, H110A, Y209F, and W219A) could be readily detected by the quenching of alrestatin fluorescence. The pattern obtained with the C298A mutant (not shown) is practically identical to that displayed for the wild-type enzyme in Figure 4A, and the alrestatin dissociation constant in the presence of NADP$^+$ is identical for these two enzymes (Table 1).

In the H110A, Y209F, and W219A mutants, quenching of alrestatin upon binding to the enzyme/NADP$^+$ complex was also evident from the nonlinear upward curvature of the

Table 2: Binding of Alrestatin to Aldose Reductase Determined by Ultrafiltration Assays[a]

	fraction of free alrestatin				
coenzyme	wild-type	Y48H	Y48F	W20A	H110A
no coenzyme	0.73	0.90	1.01	1.01	1.01
10 μM NADPH	0.43	0.92	1.02	1.00	0.96
10 μM $NADP^+$	0.09	0.87	0.97	0.97	0.22

[a] One-milliliter assays were analyzed for free alrestatin by filtering 100 μL through a Centricon 3 (Amicon) ultrafiltration membrane (MW cutoff = 3 kDa). The concentration of alrestatin in the filtrate was determined from its fluorescence at excitation and emission wavelengths of 340 and 380 nm, respectively. The assays contained 12 μM enzyme, 5 μM alrestatin, and coenzyme.

titration curves (shown for H110A in Figure 4C, lower panel). However, the ΔF titration curve (Figure 4C, upper panel) did not reach saturation at alrestatin levels of up to 15 μM, which indicates a decreased affinity for alrestatin as compared to the wild-type enzyme. A binding constant could not be properly determined since a saturation curve is required to obtain ΔF_{max} in eq 2. At alrestatin concentrations above 15 μM, the signal was not linear with concentration due to an inner filter effect. Furthermore, as titration proceeds to high alrestatin concentrations, the difference between the fluorescence signal with and without enzyme (=ΔF on the y-axis in Figure 4) becomes unreliable as it is a small difference between two large numbers. The displacement of the alrestatin titration curve in the presence of NADPH relative to that in its absence (apoenzyme only, Figure 4C) suggests weak binding of alrestatin to the enzyme/NADPH complex. The plots of alrestatin fluorescence quenching for the Y209F and W219A mutants were similar to that of the H110A mutant shown in Figure 4C. We thus conclude that H110A, Y209F, and W219A bind alrestatin in the presence of $NADP^+$, albeit with a reduced affinity as compared to the wild-type enzyme (Table 1).

In contrast, binding of alrestatin by the Tyr48 mutants, Y48H and Y48F, and the Trp20 mutant, W20A, could not be detected within the sensitivity of the methods used (Table 1). Alrestatin fluorescence is not quenched when it is added to the enzyme/$NADP^+$ complex, as is evident from the superimposed positions of the curves for the titration of alrestatin to buffer or enzyme (shown for Y48H in Figure 4B, lower panel). The ultrafiltration binding assays confirm that these mutants do not bind alrestatin to a significant degree (see below).

We have used the ultrafiltration assays to qualitatively determine whether the absence of alrestatin quenching upon binding to the Y48F and W20A mutants is due to an inability of these mutants to bind alrestatin. Table 2 shows that, compared to the wild type, the fraction of free alrestatin in the presence of the enzyme/$NADP^+$ complex of these mutants is high, confirming their low binding affinity for alrestatin. The degree of alrestatin binding to each enzyme correlated well with the degree of enzyme inhibition by this compound (Table 1). However, the ultrafiltration assay suggests that the Y48H mutant may bind alrestatin weakly, a result which is not detected by the spectroscopic method (Table 1). The marginal binding of alrestatin by Y48H detected by the ultrafiltration assay (free fraction of alrestatin = 0.87) is consistent with the very weak inhibition of this mutant enzyme by alrestatin (20% at 100 μM alrestatin).

Table 2 also shows that the enzyme/$NADP^+$ complex of the H110A mutant binds alrestatin, although the binding appears to be weaker as compared to the wild-type enzyme.

Table 3: Effect of Trp20 Mutation on Aldose Reductase Inhibition (IC_{50}, μM)

	wild-type	W20A
zopolrestat	0.06	30
tolrestat	0.1	>250
FK366	0.4	40
AL1576	0.8	>400
alrestatin	1	ni (75 μM)[a]
ponalrestat	1.2	>200
sorbinil	2	ni (400 μM)[a]
citrate	60 mM	60 mM

[a] ni = no inhibition at indicated maximal concentration used.

The H110A mutant binds alrestatin in the presence of the reduced coenzyme, NADPH, only very weakly or not at all. Whereas the displacement of the fluorescence titration curve in the presence of NADPH relative to that with buffer suggests some binding (Figure 4C, lower panel), no significant binding could be detected by the ultrafiltration assay (Table 2).

Effect of Tryptophan-20 Mutation on the Activity of Various Aldose Reductase Inhibitors. Table 3 shows the IC_{50} values of various aldose reductase inhibitors tested on freshly prepared recombinant human aldose reductase enzyme. Assuming pure noncompetitive inhibition of wild-type aldose reductase by these compounds, the IC_{50} is equal to K_i (see above, where K_{ii} is shown to be not significantly different from K_{is} and hence $K_i = K_{is} = K_{ii}$ for the inhibition by alrestatin) and does not depend on substrate concentration but rather on enzyme concentration due to the rather tight binding of the inhibitor/enzyme complex (low K_i). Therefore, the same enzyme concentration (0.5 μM) was used in all cases for all inhibitors. Thus, even though the assumption of pure noncompetitive inhibition in the case of the W20A mutant may conceivably be in error, the fact that a saturating DL-glyceraldehyde concentration was not reached should make the inhibition of the W20A mutant enzyme more apparent, i.e., lower the IC_{50}.

The compounds are listed according to their inhibitory potency, and mostly demonstrate IC_{50}s in the submicromolar/micromolar range. As shown earlier, citrate inhibits aldose reductase in the millimolar range (Harrison et al., 1994). The inhibitory potency of the commercially developed micromolar range alrestatin-like aromatic inhibitors (Figure 5) is reduced several hundredfolds (100–2500-fold, mean >800-fold) when tested against the W20A mutant enzyme. In the case of alrestatin and sorbinil, no inhibition could be demonstrated at the maximal concentrations of the two compounds that could be used. The inhibition of the W20A mutant by citrate, which lacks an aromatic ring system, is similar to that seen in the wild-type enzyme.

DISCUSSION

These studies were undertaken to determine the effect of mutations in human aldose reductase active-site residues on the binding of the $NADP^+$/NADPH nucleotides and aldose reductase inhibitors. The binding of coenzymes to aldose reductase produces spectroscopic effects which are not usually found in dehydrogenases upon binding of the nicotinamide adenosine coenzymes. It was previously shown that the NADPH fluorescence emission intensity is reduced to approximately 80% upon binding to the bovine aldose reductase (Grimshaw et al., 1990b). In the human enzyme, an even larger reduction to about 40% is found (Table 1). In most dehydrogenases, the fluorescence intensity of NAD(P)H is not quenched, but is enhanced severalfold upon binding to the

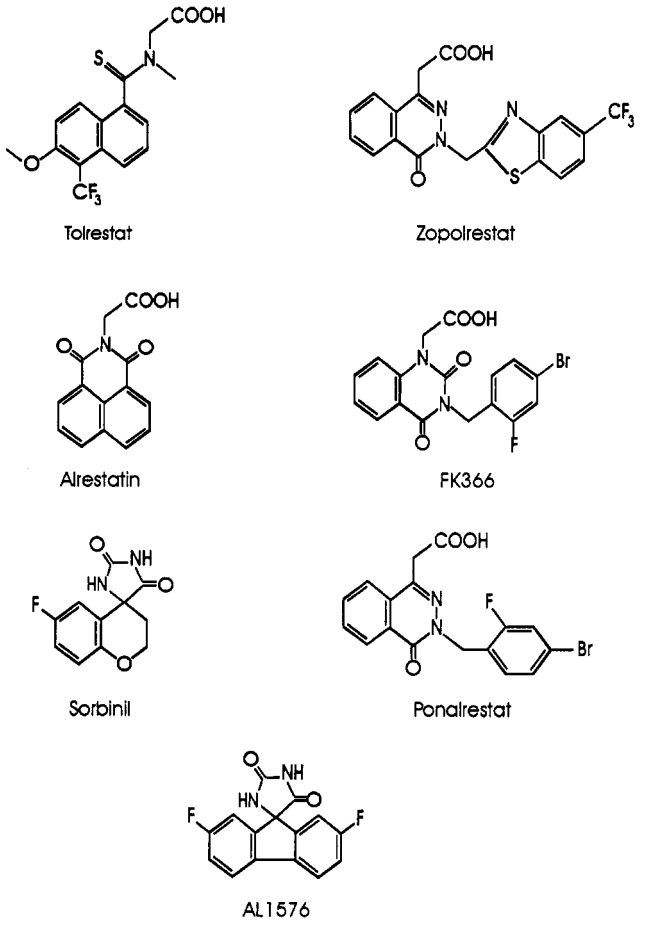

FIGURE 5: Structures of various aldose reductase inhibitors used in this study.

enzyme. This is usually explained by the separation of the nicotinamide and adenine rings in the bound state, whereas in solution the two rings are stacked, leading to fluorescence quenching (Lakowicz, 1983). In addition, partial shielding from solvent in the bound state has been implicated in the fluorescence increase (Visser, 1987). Inspection of the crystallographic structure of aldose reductase (Wilson et al., 1992; Harrison et al., 1994) suggests that similar mechanisms may also be operative to enhance the fluorescence intensity of bound NADPH. The observed opposite behavior appears to be mediated by the side chains of His110, Tyr48, and Trp20, since mutation of each of these residues increases the NADPH emission intensity (Table 1). The mechanism by which His110, Tyr48, and Trp20 quench NADPH fluorescence is not clear. Given the fact that these residues are all within 5 Å of the nicotinamide ring (Wilson et al., 1992; Harrison et al., 1994), collisional quenching, exciplex formation, or steric effects inducing a constrained conformation of NADPH with low intrinsic fluorescence might be involved.

A second interesting feature related to coenzyme binding is the appearance of a charge-transfer band upon binding of $NADP^+$ to aldose reductase (Figure 1, Table 1), which has previously been observed in the bovine enzyme (Grimshaw et al., 1990b). This band most likely originates from the nicotinamide portion of the coenzyme, since it is susceptible to charge-transfer reactions (Rizzo et al., 1987), and is present in several mutants investigated, although with varying intensity (Table 1). It is not clear which interactions between coenzyme and protein are responsible for its existence. It is interesting to note that quenching of bound NADPH (Velick, 1958) and the appearance of a charge-transfer band with an extinction coefficient of 1000 M^{-1} cm^{-1} at 360-nm wavelength (Kirschner et al., 1971) are also found in glyceraldehyde-3-phosphate dehydrogenase. It is not known whether these similarities are caused by any structural determinants which are common to these enzymes.

A general concern of mutagenesis studies is that a mutation results in a gross perturbation of the overall protein structure. The binding constants of the $NADP^+$/NADPH coenzymes to the wild-type and various mutant enzymes are quite comparable and consistent with proper folding of the proteins and a similar structure for the active-site center and coenzyme binding site, and argue for an overall protein folding similar to that of the wild-type enzyme (Table 1). In particular, the completely inactive Y48F mutant and the slightly active Y48H and H110A mutants have comparable coenzyme binding constants to the wild-type enzyme. Furthermore, the preservation of the $NADP^+$ charge-transfer band in the mutant enzymes is consistent with a similar interaction of oxidized nicotinamide with the protein as in the wild-type enzyme. The recent determination of the crystal structure of the Y48H mutant confirms a nearly identical structure as the wild-type enzyme except for the immediate surroundings of His48 in the mutant active site (Bohren et al., 1994).

In addition to the binding of coenzymes, we also investigated the binding of the inhibitor alrestatin to aldose reductase. Alrestatin, 1,3-dioxo-1*H*-benz[de]isoquinoline-2(3*H*)-acetic acid, was the first orally active aldose reductase inhibitor shown to be effective in controlling polyol accumulation and preventing cataract formation in galactosemic and diabetic rats (Dvornik et al., 1973), and the first to be introduced in humans (Gabbay et al., 1979). The fluorescence excitation/emission and quenching characteristics of this compound upon binding to aldose reductase made it ideal for performing these binding studies.

Until recently, there has been ambiguity in the interpretation of steady-state aldose reductase enzyme inhibition kinetics. There is general agreement that the inhibition pattern is uncompetitive or noncompetitive as indicated by a large intercept effect with respect to aldehyde substrates (Bhatnagar et al., 1990; O'Brian et al., 1982; Kador & Sharpless, 1978). The pattern of alrestatin inhibition of aldose reductase shown in this study, i.e., competitive versus the alcohol substrate xylitol and noncompetitive versus the aldehyde substrate D-xylose (Figure 3A,B), is similar to that demonstrated for aldose reductase inhibition by citrate (Harrison et al., 1994) and sorbinil (Liu et al., 1992). It was recently pointed out that in the ordered Bi-Bi mechanism of aldose reductase, these inhibition patterns could be explained if the inhibitor were to bind preferentially to the enzyme/$NADP^+$ complex (Liu et al., 1992; Ward et al., 1993). The uncompetitive/noncompetitive pattern of inhibitor *vs* aldehyde follows from Cleland's rule that a dead-end inhibitor makes an "intercept effect", i.e., an uncompetitive to noncompetitive inhibition if it combines with an enzyme complex downstream of the varied substrate (Segel, 1975).

A direct demonstration that alrestatin binds preferentially to the enzyme/$NADP^+$ complex is provided in this study by fluorescence titration assays (Figure 4) and by assaying the fraction of unbound alrestatin by ultrafiltration (Table 2). The preferential binding of alrestatin to the enzyme/$NADP^+$ form suggests a direct interaction between alrestatin and the positively charged nicotinamide of $NADP^+$. By X-ray crystallography, we have recently identified a positively charged anion site which binds a carboxylate of citrate (Harrison et al., 1994). Preferential binding of citrate to the enzyme/$NADP^+$ form ($Asp43^-$/$Lys77^+$/$Tyr48^0$/$NADP^+$, at

the nicotinamide ring) as opposed to the enzyme/NADPH form (Asp43$^-$/Lys77$^+$/Tyr48^0/NADPH, at the nicotinamide ring) was deduced from its steady-state inhibition pattern (see above). It is also consistent with our previous finding that the nucleotide present in the aldose reductase crystals is NADP$^+$ (Harrison et al., 1994). It is important to note that the hitherto unidentified electron density present in the active-site pocket of aldose reductase is displaced and disappears when the enzyme is crystallized in a complex with the more potent and more avidly bound aldose reductase inhibitor zopolrestat (Wilson et al., 1992; Wilson et al., 1993). The unidentified electron density, apparently also found in a 1.4-Å refined crystal structure (Wilson et al., 1993), was recently identified as citrate (Harrison et al., 1994) which is present in the crystallization media. The carboxylate moiety of zopolrestat was described as being located at a position that appears to be identical to the binding site of the carboxylate of the citrate and the binding sites of cacodylate and glucose 6-phosphate (Harrison et al., 1994).[3] It is likely that the carboxylate of alrestatin also binds to the anion well in the active site.

Since it is very likely that alrestatin is anchored via its negatively charged carboxylate into the anion well in the enzyme/NADP$^+$ complex, we sought to more fully characterize its binding avidity. We investigated several enzymes with mutations of specific neighboring residues in the active-site pocket. Mutation of the His110 residue (H110A), previously shown to direct substrate stereochemical specificity, mildly affected alrestatin binding and inhibition. The mutation of Cys298 (C298A) had no marked effect on alrestatin binding or inhibition, while mutation of the nicotinamide-stacking Tyr209 (Y209F) and the Trp219 (W219A) mutant affected these properties only slightly.

However, alrestatin binding was abolished in the Tyr48 mutant Y48F (Tables 1 and 2). This demonstrates the dominant role of Tyr48 in alrestatin binding and is consistent with involvement of the anion well in the binding. The Tyr48 residue was shown to be the proton donor in the catalytic reaction, and as a result the Y48F mutant is enzymatically inactive (Bohren et al., 1994). The absence of alrestatin binding to the Y48F mutant is consistent with a necessity for the hydroxyl group of Tyr48 to interact with the Asp43$^-$/Lys77$^+$ and NADP$^+$ in order to create the anion well. The Y48H mutant, on the other hand, shows no alrestatin binding by the spectroscopic method, but weak inhibition of enzymatic activity. This mutant, Y48H, has partial enzyme activity due to the presence of a water molecule hydrogen-bonded to the Nϵ2 of the mutated His48 residue. The water molecule is inserted in the exact relative location of the hydroxyl group of Tyr48 in the wild-type structure, and mediates proton transfer during catalysis in this mutant (Bohren et al., 1994). The Y48H mutant crystal structure clearly shows the citrate bound within the active site, and this mutant is inhibited by citrate as well. However, from the present study, it appears that this water molecule cannot substitute for the Tyr48 hydroxyl as far as binding of alrestatin is concerned. Interestingly, the involvement of a tyrosine residue in inhibitor binding by aldose reductase had been predicted by chemical modification studies and molecular orbital calculations of inhibitor molecules (Kador & Sharpless, 1983).

[3] Protein Data Bank reference numbers 1ACS, 1ACR, and 1ACQ for the atomic coordinates and structure factors of the citrate/-, cacodylate/-, and glucose 6-phosphate/enzyme complexes, respectively. We were unable to directly compare these binding sites with the zopolrestat/enzyme complex (Wilson et al., 1993) as the latter coordinates were embargoed by the authors.

Mutation of the Trp20 residue (W20A) markedly affected alrestatin binding and enzyme inhibition. The W20A mutation completely abolished alrestatin binding and inhibition of enzymatic activity, indicating that this residue is crucial to the binding of alrestatin. Of interest, all of the commercially developed inhibitors listed in Table 3 are affected by the W20A mutation with loss of inhibitory potency, suggesting that they all bind at the active site and arguing against an alternative or second binding site on the enzyme.

Modeling studies suggest that the alrestatin ring system stacks against the hydrophobic Trp20 residue. Inhibition by citrate, a prototype inhibitor which lacks an aromatic ring, is not affected by the Trp20 mutation since its carboxylate negative charge is sufficient to anchor it to the anion well. The binding of alrestatin and the other negatively charged (–COOH and spirohydantoin-type) inhibitors is markedly enhanced by the stacking of their aromatic ring system against the Trp20 residue (Figure 5). Thus, there appears to be two main requirements for this type of aldose reductase active-site inhibitor: (1) a negative charge on the inhibitor to anchor it to the anion well, and (2) aromatic ring systems to stabilize and increase the avidity of binding by several orders of magnitude. The static structure model of the holoenzyme/zopolrestat complex described by Wilson et al. (1993) indeed shows that the negatively charged carboxylate of zopolrestat is located within the active site identically[3] to the location we described for the carboxylate of citrate (Harrison et al., 1994). One of the aromatic double rings of zopolrestat is stacked against Trp20, and the other against Trp111, with numerous interactions with other hydrophobic residues lining the active-site pocket. The binding of tolrestat, AL1576, alrestatin, and sorbinil (Figure 5), all containing a single aromatic ring system, is dramatically affected by mutation of the Trp20 residue (no inhibition or >500-fold reduction in IC_{50}s). Zopolrestat, FK366, and ponalrestat are less affected by this mutation (100–500-fold reductions in IC_{50}s), presumably because of the presence of an additional flexible aromatic pharmacophor ring system that can accommodate the active-site pocket and bind to some other hydrophobic residue (e.g., Trp111 in the case of zopolrestat). AL1576, a two aromatic ring inhibitor which is highly dependent on Trp20 for binding, is an exception in that it has an inflexible double aromatic ring system that behaves as one.

These studies describe and explain the minimum requirements for the design of potent aldose reductase inhibitors that interact with the active site. Clearly, without prior knowledge of the crystal structure of aldose reductase or its active-site pocket, the pharmaceutical industry has developed some excellent potent inhibitors that admirably fulfill these requirements. It remains to be determined whether the lack of therapeutic effectiveness and side effects of such inhibitors in humans is due to inhibitor nonspecificity, inappropriate targetting of the inhibitors to the active site, or an inadequate understanding of the biology and pathogenetic mechanisms of aldose reductase.

REFERENCES

Bhatnagar, A., Liu, S., Das, B., Ansari, N. H., & Srivastava, S. K. (1990) *Biochem. Pharmacol. 39*, 1115–1124.

Bohren, K. M., & Gabbay, K. H. (1993) in *Enzymology and Molecular Biology of Carbonyl Metabolism* (Weiner, H., Crabb, D. W., & Flynn, T. G., Eds.) Vol. 4, pp 267–277, Plenum, New York.

Bohren, K. M., Bullock, B., Wermuth, B., & Gabbay, K. H. (1989) *J. Biol. Chem. 264*, 9547–9551.

Bohren, K. M., Page, J. L., Shankar, R., Henry, S. P., & Gabbay, K. (1991) *J. Biol. Chem. 266*, 24031–24037.
Bohren, K. M., Grimshaw, C. E., Lai, C.-J., Harrison, D. H., Ringe, D., Petsko, G. A., & Gabbay, K. H. (1994) *Biochemistry 33*, 2021–2032.
Borhani, D. W., Harter, T. M., & Petrash, J. M. (1992) *J. Biol. Chem. 267*, 24841–24847.
Cantor, C. R., & Schimmel, P. R. (1979) *Biophysical Chemistry. Part I: The Conformation of Biological Macromolecules*, pp 266–272, W. H. Freeman, New York.
Chylack, L. T., Henriques, H. F., & Cheng, H.-M. (1979) *Ophthalmology 86*, 1579–1585.
Dvornik, D. (1987) *Aldose Reductase Inhibition* (Porte, D., Ed.) McGraw-Hill, New York.
Dvornik, D., Simard-Duquesne, N., Sestanj, M. K., Gabbay, K. H., Kinoshita, J. H., Varma, S. D., & Merola, L. O. (1973) *Science 182*, 1146–1148.
Fukushi, S., Merola, L. O., & Kinoshita, J. H. (1980) *Invest. Ophthalmol. Visual Sci. 3*, 313–315.
Gabbay, K. H. (1973) *N. Engl. J. Med. 288*, 831–836.
Gill, S. C. & vonHippel, P. H. (1989) *Anal. Biochem. 182*, 319–326.
Grimshaw, C. E. (1992) *Biochemistry 31*, 10139–10145.
Grimshaw, C. E., Shahbaz, M., & Putney, C. G. (1990a) *Biochemistry 29*, 9947–9955.
Grimshaw, C. E., Shahbaz, M., & Putney, C. G. (1990b) *Biochemistry 29*, 9936–9946.
Harrison, D. H., Bohren, K. M., Ringe, D., Petsko, G. A., & Gabbay, K. H. (1994) *Biochemistry 33*, 2011–2020.
Hayman, S., & Kinoshita, J. H. (1964) *J. Biol. Chem. 240*, 877–882.
Kador, P. F. (1988) *Med. Res. Rev. 8*, 325–352.
Kador, P. F., & Sharpless, N. E. (1978) *Biophys. Chem. 8*, 81–85.
Kador, P. F., & Sharpless, N. E. (1983) *Mol. Pharmacol. 24*, 521–531.
Kador, P. F., Robison, W. G., & Kinoshita, J. H. (1985) *Annu. Rev. Pharmacol. Toxicol. 25*, 691–714.
Kador, P. F., Kinoshita, J. H., & Sharpless, N. E. (1986) *Metabolism 35* (Suppl. 1), 109–113.
Kinoshita, J. H. (1974) *Invest. Ophthalmol. 13*, 713–724.
Kinoshita, J. H., Fukushi, S., Kador, P., & Merola, L. O. (1979) *Metabolism 28* (Suppl. 1), 462–469.
Kirschner, K., Gallego, E., Schuster, I., & Goodall, D. (1971) *J. Mol. Biol. 58*, 29–50.
Kubiseski, T. J., Hyndman, D. J., Morjana, N. A., & Flynn, T. G. (1992) *J. Biol. Chem. 267*, 6510–6517.
Lakowicz, J. R. (1983) *Principles of Fluorescence Spectroscopy*, p 14, Plenum, New York.
Liu, S., Bhathnagar, A., & Srivastava, S. K. (1992) *Biochem. Pharmacol. 44*, 2427–2429.
Morrison, J. F. (1969) *Biochim. Biophys. Acta 185*, 269–286.
O'Brian, M. M., Schofield, P. J., & Edwards, M. R. (1982) *J. Neurochem. 39*, 810–814.
Racker, E., & Krimsky, I. (1952) *J. Biol. Chem. 198*, 731–743.
Rizzo, V., Pande, A., & Luisi, P. L. (1987) in *Pyridine Nucleotide Coenzymes: Chemical, Biological and Medical Aspects* (Dolphin, D., Poulson, R., & Avramovic, J., Eds.) Vol. I, pp 99–161, John Wiley and Sons, New York.
Segel, I. H. (1975) *Enzyme Kinetics. Behavior and Analysis of Rapid-equilibrium and Steady-state Enzyme Systems*, p 779. John Wiley and Sons, New York.
Steiner, R. F., & Kirby, E. P. (1969) *J. Chem. Phys. 73*, 4130–4135.
Stinson, R. A., & Holbrook, J. J. (1973) *Biochem. J. 131*, 719–728.
Van Heiningen, R. (1959) *Nature 184*, 194–195.
Van Heiningen, R. (1962) *Exp. Eye Res. 1*, 396–404.
Velick, S. F. (1958) *J. Biol. Chem. 223*, 1455–1467.
Ward, W. H. J., Cook, P. N., Mirrless, D. J., Brittain, D. R., Preston, J., Carey, F., Tuffin, D. P., & Howe, R. (1993) in *Enzymology and Molecular Biology of Carbonyl Metabolism* (Weiner, H., Crabb, D. W., & Flynn, T. G., Eds.) Vol. 4, pp 267–277, Plenum, New York.
Wermuth, B. (1985) in *Enzymology of Carbonyl Metabolism 2: Aldehyde Dehydrogenase, Aldo-Keto Reductase, and Alcohol Dehydrogenase* (Flynn, T. G., & Weiner, H., Eds.) pp 209–230, Alan, R. Liss, New York.
Wermuth, B., Burgisser, H., Bohren, K. M., & vonWartburg, J.-P. (1982) *Eur. J. Biochem. 127*, 279–284.
Williams, J. W., & Morrison, J. F. (1979) *Methods Enzymol. 63*, 437–467.
Wilson, D. K., Bohren, K. M., Gabbay, K. H., & Quiocho, F. A. (1992) *Science 257*, 81–84.
Wilson, D. K., Tarle, I., Petrash, J. M., & Quiocho, F. A. (1993) *Proc. Natl. Acad. U.S.A. 90*, 9847–9851.